Neuroscience Vol. 20, No. 2, pp. 637–651, 1987
Printed in Great Britain

0306-4522/87 $3.00 + 0.00
Pergamon Journals Ltd

MORPHOLOGY OF CORTICALLY PROJECTING BASAL FOREBRAIN NEURONS IN THE RAT AS REVEALED BY INTRACELLULAR IONTOPHORESIS OF HORSERADISH PEROXIDASE

K. SEMBA, P. B. REINER, E. G. MCGEER and H. C. FIBIGER
Division of Neurological Sciences, Department of Psychiatry, University of British Columbia, Vancouver, BC, Canada V6T 1W5

Abstract—The intracellular horseradish peroxidase technique was employed to study the morphology of basal forebrain neurons that were identified as cortically projecting by antidromic invasion from the cerebral cortex. Four neurons were examined in detail; they were located at different rostrocaudal levels within the basal forebrain. Their somata were large, 30–50 μm in longest dimension, and gave rise to three to eight primary dendrites, which ramified into third- to fifth-order dendrites. The longest observed dendrite in each neuron terminated at a distance of 600–900 μm from the soma. The sizes of soma and dendritic field of the two most rostrally located cells were smaller than those of the other two cells located more caudally. Dendritic spines were seen in all four cortically projecting basal forebrain neurons. Spines had shafts of variable lengths, and usually had spherical or elongated heads. The density of spines varied among the four neurons; one neuron, a type II cortically projecting basal forebrain neuron as defined physiologically by Reiner *et al.*,[37] had a much greater number of dendritic spines than the other three neurons, which were type I neurons. No somatic spines were observed. Presumptive axons were identified in three of the four cortically projecting basal forebrain neurons. These axons originated from either the soma or a primary dendrite, and two of them gave off local collaterals, which displayed occasional bouton-like swellings.

The above observations confirm and extend previous findings that cortically projecting neurons in the basal forebrain are large multipolar cells, and provide evidence to support the conclusion that these cells, although somewhat variable in size, generally have extensive dendrites which display frequent spines.

Immunohistochemical studies using antibodies directed to choline acetyltransferase (ChAT), a specific marker for acetylcholine, have shown that the basal forebrain contains a group of large cholinergic cells in a variety of species (see refs 49 and 51 for reviews). These cells are distributed in a column extending from the medial septum caudally to the vertical and horizontal limbs of the diagonal band of Broca, ventral pallidum, and ventromedial globus pallidus or the nucleus basalis.[13,20,21,29,31,40,41,42]

These basal forebrain cholinergic cells project topographically to the cerebral cortex. This projection was originally hypothesized by Shute and Lewis[47] in 1967 on the basis of acetylcholinesterase staining, and has been confirmed more recently by using tract-tracing techniques[7,17,19,24,25,36,39,53] combined with either ChAT immunohistochemistry[30,38,50,55,56] or acetylcholinesterase histochemistry,[2,12,26] or by examining cortical ChAT activity levels[28,54] or acetylcholinesterase staining[23] following basal forebrain lesions.

Morphological observations have been made on ChAT-immunoreactive[1,13,29,40] or acetylcholinesterase-containing basal forebrain neurons[16,26,33,40] as well as neurons double-labelled for retrograde markers from the cerebral cortex and either ChAT[38,50,56] or acetylcholinesterase.[12,26] However, the morphology revealed in these studies was limited to the soma and proximal dendrites. Golgi-stained material has provided more extensive morphology, revealing parts of distal dendrites as well.[6,32] However, these cells were unidentified in terms of their projections.

The intracellular horseradish peroxidase (HRP) technique permits the morphological analysis of individual neurons at a level of detail comparable to the Golgi technique, and, of course, the fundamental advantage of the intracellular HRP technique is that it allows physiological properties to be correlated with morphology.[4,22] In the present study, this technique was used to examine the morphology of physiologically identified and characterized CPBF neurons. Preliminary observations have been published in abstract form.[44]

EXPERIMENTAL PROCEDURES

Details of the experimenal procedures regarding animal preparation and recording are described elsewhere.[37] Briefly, recordings were made in 36 chloral-hydrate-anesthetized rats with micropipettes filled with 4–5% HRP in 0.05 M Tris buffer containing 0.2–0.25 M KCl (final pH adjusted to 8.5), using a high-input impedance electrometer. Direct current resistance of these electrodes was 40–60 MΩ. Cortical stimulation for antidromic activation was delivered through bipolar electrodes implanted in the frontal cortex, rostral cingulate cortex, and caudal cingulate cortex.

Address for correspondence: Kazue Semba, Division of Neurological Sciences, University of British Columbia, Vancouver, BC, Canada V6T 1W5.

Abbreviations: CPBF neuron, cortically projecting basal forebrain neuron; ChAT, choline acetyltransferase; HRP, horseradish peroxidase.

Following antidromic identification (for criteria, see Reiner *et al.*[37]) and physiological characterization, cells in the basal forebrain were penetrated intracellularly, usually using 5-msec oscillation pulses. When good penetration was obtained, as confirmed by a sudden drop of membrane potential and an increase in action potential size, HRP was iontophoresed intracellularly by applying +7-nA, 250-msec pulses at 2 Hz for 60–80 sec. Antidromic activation was monitored continuously at 1–2 Hz throughout and, when possible, following HRP iontophoresis.

One to 6 hr following intracellular HRP iontophoresis, rats were injected with heparin (1250 units, i.v.), and overdosed with chloral hydrate. Transcardiac perfusion was initiated with cold phosphate-buffered saline (about 50 ml) followed by 300–400 ml fixative containing 3% paraformaldehyde and 1% glutaraldehyde in 0.1 M sodium phosphate buffer (pH 7.4). Following perfusion, the brain was removed and postfixed in the same fixative for 2 hr at 4°C, and then placed in 15% sucrose in 0.1 M phosphate buffer at 4°C overnight. The tissue was blocked and cut into 100-μm coronal sections on a freezing microtome. Histochemical reaction, using diaminobenzidine as a chromagen with cobalt intensification, was performed as described elsewhere[43] for light microscopy, except that, in the present study, the concentrations of cobalt chloride and hydrogen peroxide were 0.1 and 0.0016%, respectively. Following the histochemical reaction, some sections were counterstained with Cresyl Violet.

Camera lucida drawings of sections containing HRP-labelled neurons were made with a drawing tube attached to a microscope at the magnification of ×400. Each HRP-labelled neuron was reconstructed by superimposing these camera lucida drawings. Some end sections which could not be unequivocally related to adjacent sections were excluded from the final reconstructions. However, some unconnected labelled processes were included if a majority of the labelled processes in the same section could be clearly connected with labelled elements in the adjacent section.

Measurements of somal size were made on camera lucida drawings. Dorsoventral and mediolateral extents of the dendritic field were measured in straight lines from the composite camera lucida drawings of the entire neuron. Rostrocaudal extent of each HRP-labelled neuron was estimated from the number of 100-μm sections containing its dendrites. No correction was made for tissue shrinkage.

Dendritic arborization of labelled cells was analysed according to Sholl[46] as adopted by Shaw and Baker.[45] First, the mediolateral and dorsoventral position of the soma was marked on each individual unreconstructed camera lucida drawing of an HRP-labelled neuron, and concentric circles spaced 100-μm apart were drawn. In the drawing containing the soma of the labelled neuron, the number of dendrites intersected by a circle of 100-μm radius centering the soma was counted and the number represented the number of dendrites intersected by an approximate sphere of 100-μm radius. In order to obtain an estimate of the number of dendrites intersected by an approximate sphere of 200-μm radius, the number of intersected dendrites was counted for a circle of 200-μm radius in the section with the cell body. To this number was added the number of dendrites intersected by a circle of 100-μm radius on the camera lucida drawings of (100-μm) sections immediately above and below the section containing the soma. The sum was then taken as the number of dendrites intersected by an approximate sphere of 200-μm radius. This iterative procedure was continued as far as dendrites could be followed. The presumptive axons and their collaterals were excluded from this analysis. The criteria for identification of an axon were: (1) relatively constant width, and (2) smooth surface without obvious protuberances.

The distribution of spines as a function of radial distance from the soma was analysed similarly, by using the same set of concentric circles drawn on camera lucida drawings. Individual spines were counted in the microscope at the magnification of ×400. The number of spines counted between the soma and the radius of 100 μm was assigned to the sphere of 100-μm radius, etc.

To examine spine density as a function of radial distance from the soma, an index was obtained by dividing the spine count by the number of dendrites intersected. While this "spine density" index does not represent the absolute spine density, it indicates the concentration of spines as a function of distance from the soma which is approximately normalized in terms of the number of dendrites.

RESULTS

A total of 39 cortically projecting basal forebrain (CPBF) neurons were studied physiologically using HRP-filled electrodes; 20 of the 39 were successfully penetrated and HRP was iontophoresed intracellularly. Of the 20 CPBF neurons, eight were recovered, and four of the eight were sufficiently labelled to permit detailed morphological analysis. Upon penetration, the membrane potential dropped by 10–30 mV; intracellular action potentials were 10–20 mV in size. The four cells were recovered in four different rats and will be referred to as cells 1, 2, 3 and 4. Each neuron was recovered over 5–10 sections and reconstructed from 5 to 7 sections (Figs 1–4). Morphological features of the four neurons are summarized in Table 1, along with their physiological properties [their physiological data are included with the data in the companion paper (Reiner *et al.*[37]) and, in part, presented in Fig. 2 (cell 2) and Fig. 4 (cell 4) of that paper].

Location

Cell 1 was located at the border between the globus pallidus and internal capsule, within the area often called the magnocellular basal nucleus[2,26,40] (Fig. 5A). Cell 2 was found slightly more rostrally, in the ventral forebrain at the level of the supraoptic nucleus, i.e. in the area often called the magnocellular preoptic area[40,48] (Fig. 5B). Both cell 3 (Fig. 5C) and cell 4 (Fig. 5D) were located within the same general region as cell 2, but further rostrally at the level of the decussation of the anterior commissure, in the area alternately termed the magnocellular preoptic area[40,48] or the horizontal limb of the diagonal band.[29,35]

Somata

Both cell 1 (Figs 1, 6A) and cell 2 (Fig. 2) had elongated triangular somata, 52 and 42 μm in longest dimension, respectively. Cell 3 had a smaller, L-shaped soma, 33 μm in longest dimension (Fig. 3), whereas cell 4 had an oval soma, 33 μm in longest dimension (Fig. 4).

Dendritic branching

The CPBF neurons had 3–8 primary dendrites, which left the soma mostly at its angular portions. Primary dendrites were 1–2 μm in width, and distally ramified into the third- to the fifth-order dendrites. Dendrites usually became thinner as they branched;

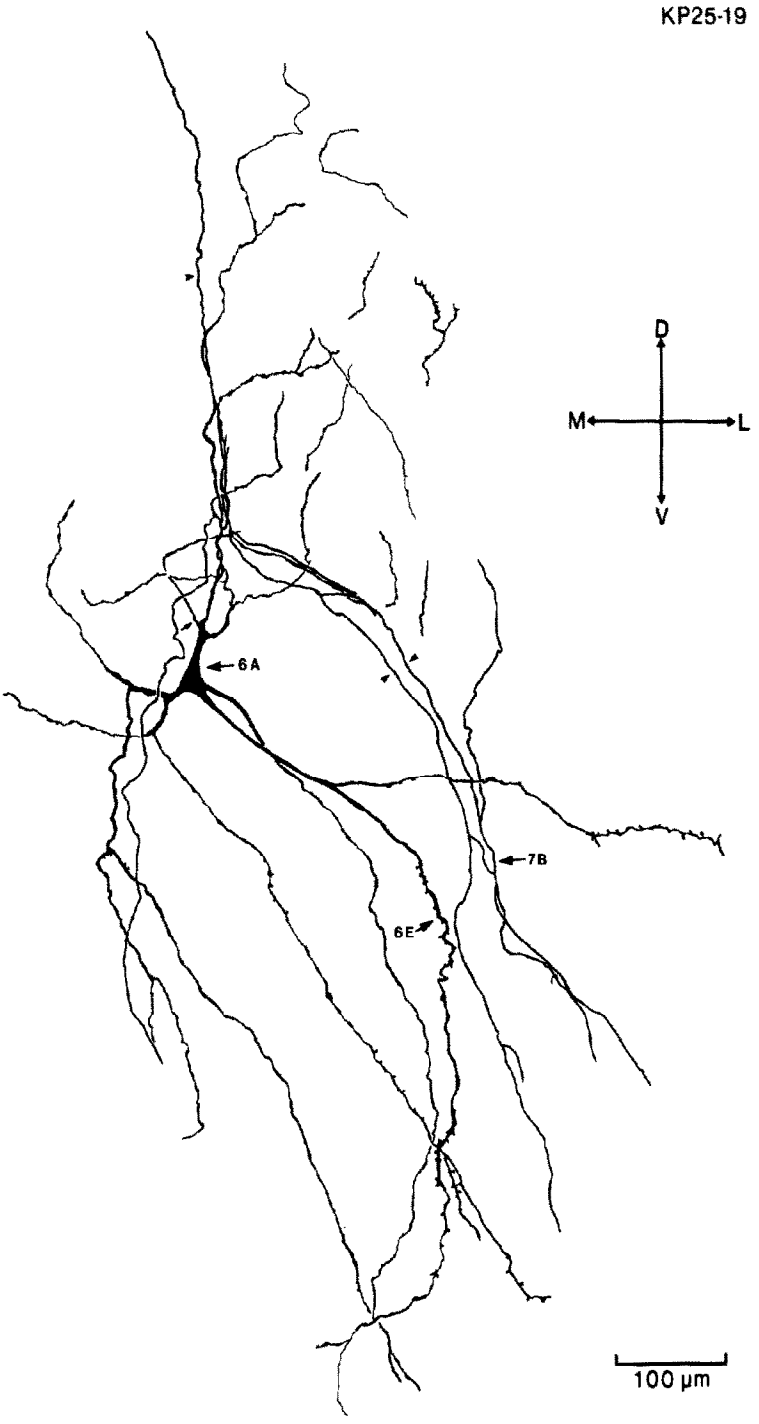

Fig. 1

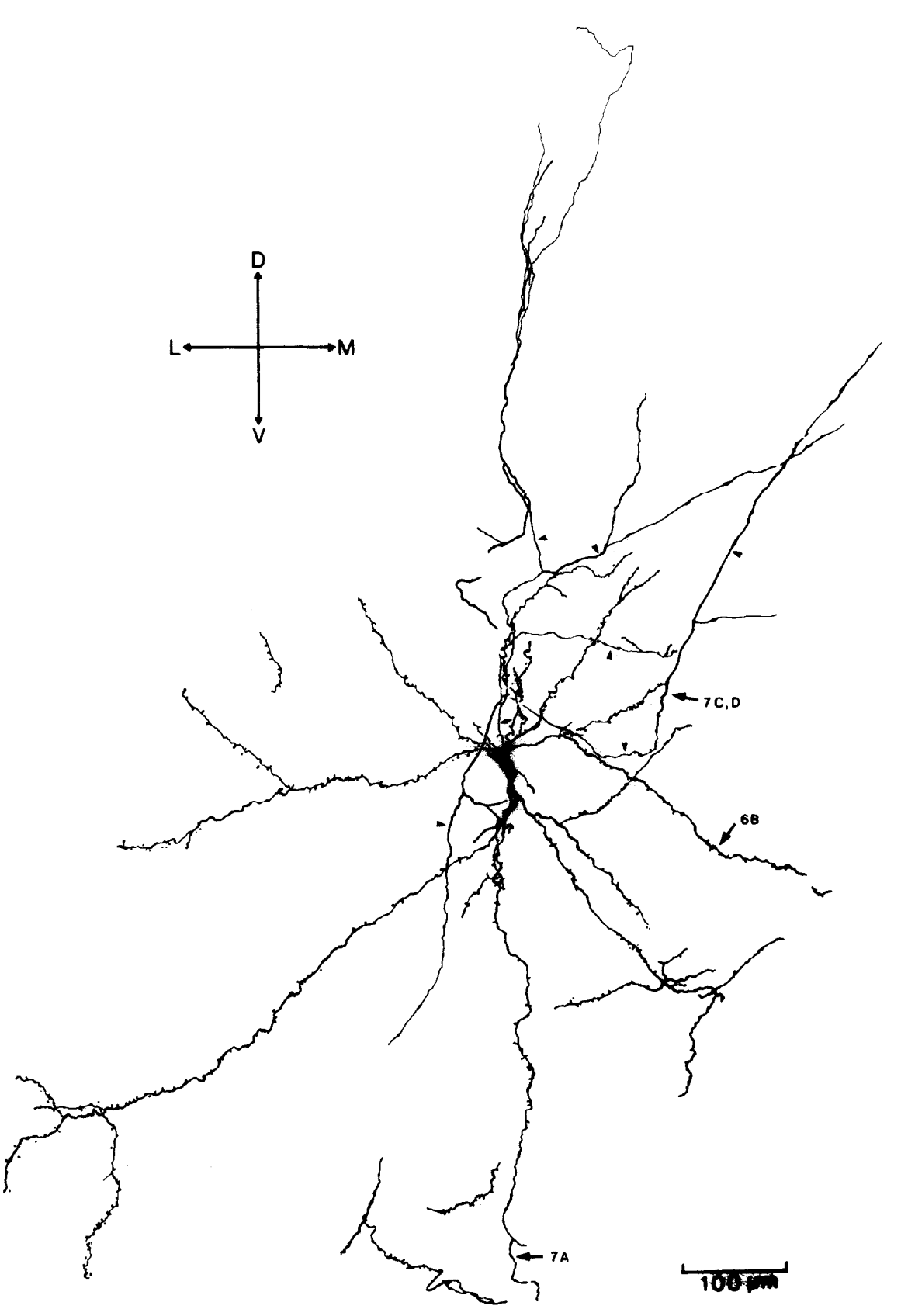

Fig. 2

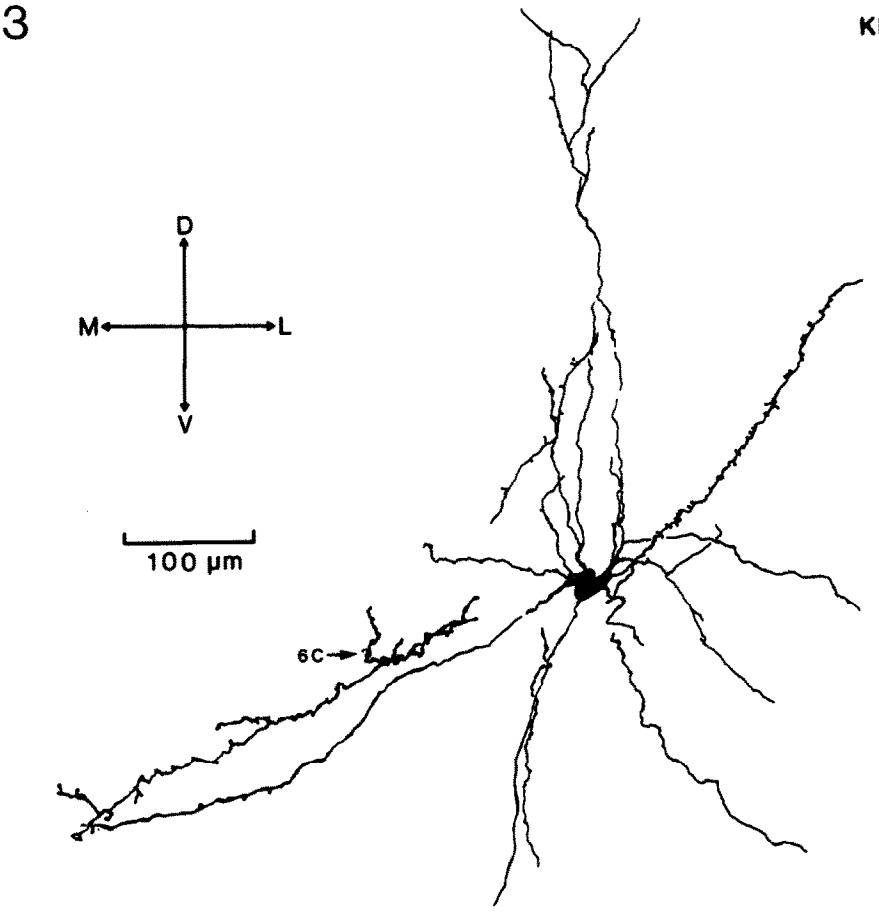

Fig. 3

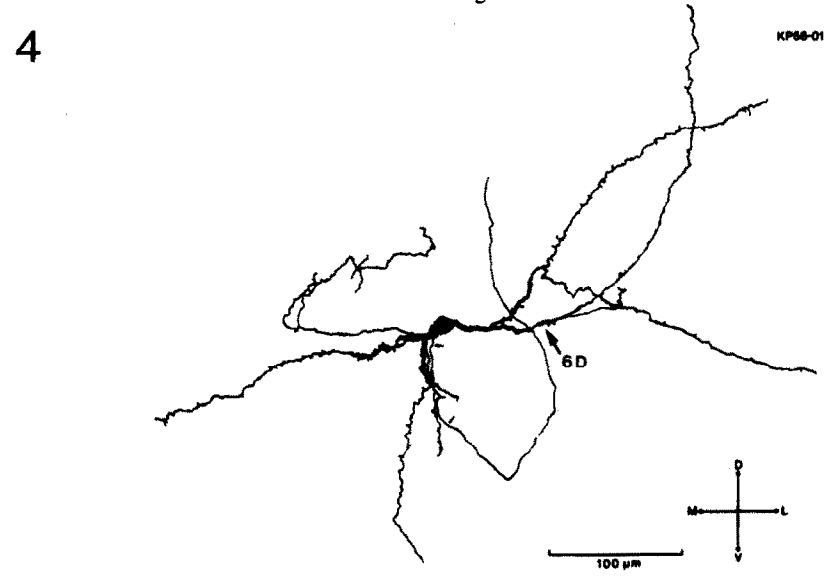

Fig. 4

Figs 1–4. Four HRP-labelled cortically projecting neurons in the basal forebrain (cells 1–4) are shown in Figs 1–4. Cells 1–4 were reconstructed from camera lucida drawing of 7, 7, 5 and 6 consecutive 100-μm sections, respectively. Some unconnected neuronal labelled elements are included in the reconstructions because a majority of labelled segments in the same section could be connected to adjacent camera lucida drawings. The smaller arrows indicate the presumptive axons (the axon could not be identified in cell 3, shown in Fig. 3), and arrowheads indicate branches of the presumptive axons. The portions of the neurons indicated by the larger arrows are shown in micrographs in the figures of the numbers accompanied by the arrows. The anatomical locations of the somata of these neurons are shown in Fig. 5. D, dorsal; V, ventral; M, medial; L, lateral.

Table 1. Summary of morphological and physiological characteristics of cortically projecting basal forebrain neurons

	Cell 1	Cell 2	Cell 3	Cell 4
Topography:				
Location of soma	Globus pallidus–internal capsule border	Magnocellular preoptic area	Magnocellular preoptic area/horizontal limb of the diagonal band	Magnocellular preoptic area/horizontal limb of the diagonal band
Cortical stimulation site	Caudal cingulate	Rostral cingulate	Rostral cingulate	Frontal
Morphology:				
Longest dimension of soma	52	42	33	28
Number of primary dendrites	5	5	8	3
Number of dendrites at the peak of branching	9	14	11	6
Highest order of dendritic branching	5th	4th	3rd	4th
Longest observed dendritic length (μm)	903	797	642	610
Dendritic tree expansion: dorsoventral (μm)	1090	830	685	415
mediolateral (μm)	645	895	620	495
rostrocaudal (μm)	600	600	500	900
Total number of observed spines	177	783	186	110
Physiology:				
Neuron type according to Reiner *et al.*[37]	Type I	Type II	Type I	Type I
Antidromic latency (msec)	7.0	17.5	10.0	2.6, 11.5
Highest frequency followed (Hz)	500	333	333	200
Spontaneous firing rate (Hz)	17.9	—	5.1	6.7

Cells 1–4 correspond to cells KP25-19, KP16-06, KP17-01 and KP56-01 in the companion paper by Reiner *et al.*[37]
For the definitions of morphological characteristics, see Experimental Procedures.

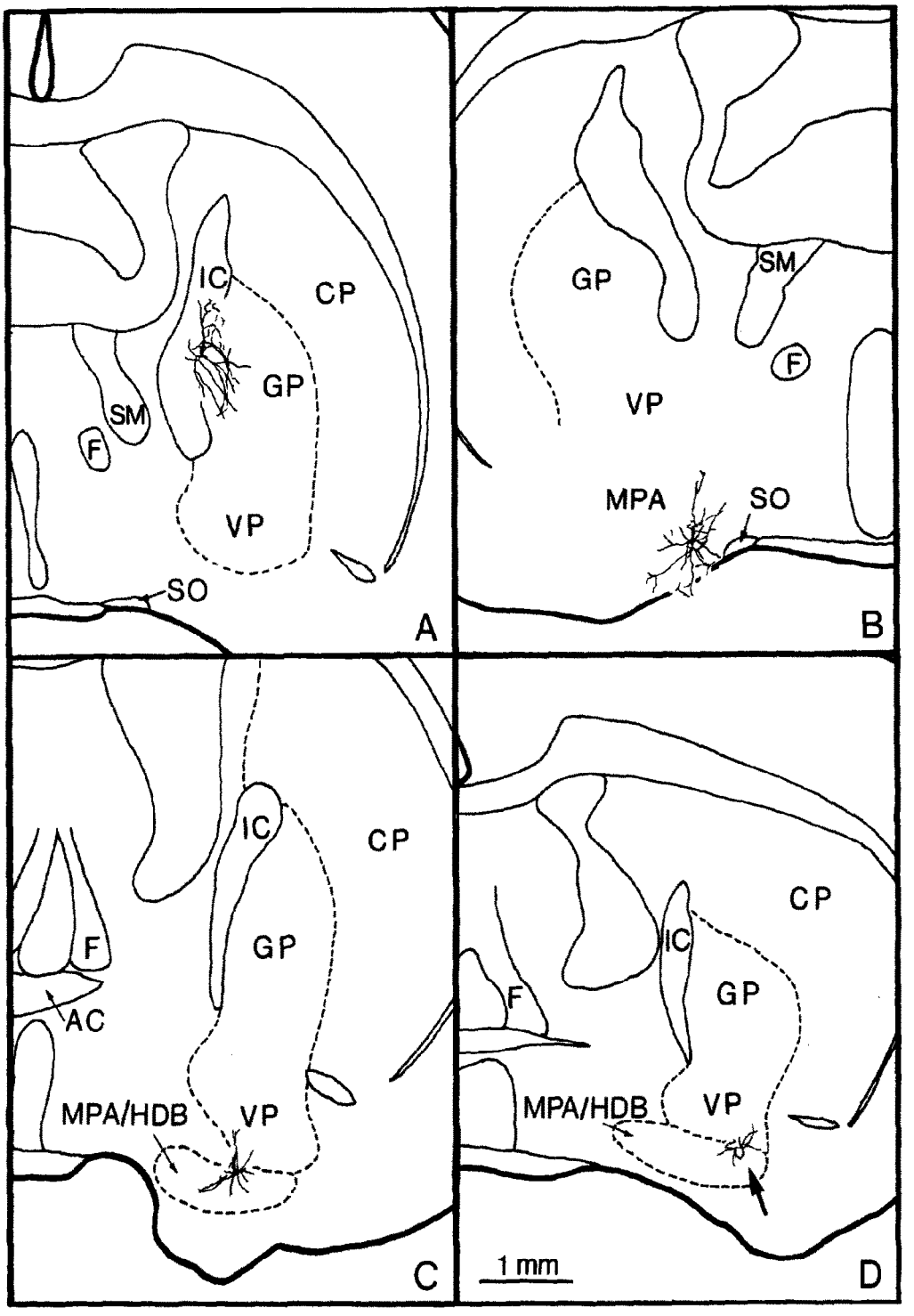

Fig. 5. Locations of the somata of four cortically projecting basal forebrain neurons labelled intracellularly with HRP. (A) cell 1, (B) cell 2, (C) cell 3, (D) cell 4. In each panel, a composite camera lucida drawing that is reduced to the corresponding magnification is superimposed on a drawing of the section containing the soma of the same cell. Note that each of the composites was based on several consecutive sections, and only a portion of the neuronal segments in the composite drawing actually appeared in the section containing the soma. As a result, in (B) some distal dendrites appear to extend beyond the ventral boundaries of the brain. These dendrites did not in fact extend beyond the pial surface (Fig. 7A), but appear so in (B) because the level of ventral surface of the brain changes through serial sections. The scale bar shown in (D) applies to all panels. AC, anterior commissure; CP, caudate putamen; F, fornix; GP, globus pallidus; HDB, horizontal limb of the nucleus of the diagonal band; IC, internal capsule; MPA, magnocellular preoptic area; SM, stria medullaris; SO, supraoptic nucleus; VP, ventral pallidum.

however, dendritic width was relatively constant between branching points. Although most dendrites had parallel linear envelopes, there were some dendrites or dendritic segments which appeared either beaded or extremely curly.

The pattern of dendritic branching was analysed numerically by employing the Sholl analysis (Fig. 8A). Of the four cells, cell 2 displayed the highest degree of dendritic branching, with five primary dendrites branching into 14 dendrites within 300 μm from the soma. Further distally, the number of dendrites gradually decreased. In cells 3 and 4, the peak of dendritic branching was less prominent, and also occurred more proximally, within 200 μm from the soma. Cells 3 and 4 had eight and three primary dendrites, respectively, which ramified into 11 and six dendrites. Cell 1 had five primary dendrites, and the number of dendrites fluctuated between five and nine within the region up to 600 μm from the soma; further distally, the number of dendrites decreased gradually.

Size of dendritic field

The extent of dendritic field in each cell, as indexed by the straight line length of the longest observed dendrite, was obtained by using the same concentric circles as those for the Sholl analysis. This length was 903, 797, 642 and 610 μm, respectively, for cells 1, 2, 3 and 4, and was correlated with the cell's somal size ($r = 0.997$, $df = 2$, $P < 0.005$).

Dorsoventral, mediolateral, and rostrocaudal extents of the dendritic field ranged 415–1090, 495–830 and 500–900 μm, respectively (Table 1). Although the shape of dendritic field varied among the four neurons (see below), the "volume" of dendritic field (estimated by multiplying the lengths of 3 extents) was roughly correlated with the radial distance of the longest observed dendrite as revealed by the Sholl analysis; the "volume" was about twice as great in cells 1 and 2 as in cells 3 and 4.

Shape of dendritic field

The shape of the dendritic field was different among CPBF neurons. In cell 1, located at the globus pallidus–internal capsule border, the dendritic field was elongated dorsoventrally (Fig. 1). Ventral to the soma, the dendritic field was extremely skewed in the ventrolateral direction, i.e. towards the center of the globus pallidus. Although the cell was essentially multipolar, some of the dendrites which left the soma on the side of the internal capsule turned towards, and entered the globus pallidus, coursing in a parallel array with the dendrites that left the soma on the side of the globus pallidus. Dorsal to the soma, there were fewer dendrites, which were also shorter than those in the ventral portion of the dendritic field. In both ventral and dorsal portions of the dendritic field, some dendrites coursed through the internal capsule. The dendrites entering the globus pallidus often passed through small fiber bundles in this area, and some of these dendrites displayed spines.

Cell 2, located more rostrally and also more ventrally in the basal forebrain (Fig. 5B), displayed more or less radially oriented dendrites, except that dorsally oriented dendrites were generally shorter than those oriented ventrally (Fig. 2). Some of the ventrally oriented dendrites appeared to reach the ventral surface of the brain (Fig. 7A). The dendritic field of cell 3 was also more-or-less radially oriented (Fig. 3), whereas that of cell 4 was somewhat flattened in the medioventral to dorsolateral orientation (Fig. 4).

Spines

Dendritic spines were seen in all the four CPBF neurons. Spine morphology varied considerably; spines had short or long shafts, typically with spherical or oval, but sometimes angular heads of variable size (Fig. 6B, D). In one instance, a Y-shaped shaft was seen with one head on each arm (Fig. 6C). In addition, dendritic appendages which appeared like spines without heads were occasionally seen, particularly in cell 1 (Fig. 6E). These appendages were included in the spine counts described below. No somatic spines were seen.

The number of spines seen in each neuron varied. Cell 2 displayed by far the greatest number of spines (783) whereas cell 1 had only 177, despite its comparable dendritic field size. In cells 3 and 4, which had smaller dendritic fields, the spine counts were 186 and 110.

The pattern of spine distribution in each neuron was numerically analysed by using the same approximate concentric spheres as those used for the Sholl analysis of dendritic branching (Fig. 8B). In general, spines were infrequent within 100 μm from the soma. Distally, spine counts increased and peaked between 200 and 600 μm from the soma among the four cells.

The pattern of "spine density", an index of relative spine density which is normalized for the number of dendtrites, was different among the four neurons (Fig. 8C). Cell 2 displayed a generally higher "spine density" than the other three neurons. Furthermore, in cell 2 there was a trend of linear increase in "spine density" towards the periphery of the dendritic field. A similar trend was seen in cell 1 as well, although the overall "spine density" was much lower than that of cell 2. In cell 3, the "spine density" peaked between 200 and 300 μm from the soma, whereas in cell 4, "spine density" remained at more or less the same level throughout its dendritic field.

Axons

Except for in cell 3, presumptive axons could be identified, originating from either the soma, as in cell 4 (Fig. 4), or a proximal dendrite, as in cell 2 (Fig. 2). In cell 1, the presumptive axon arose from a transitional zone from the soma to a primary dendrite (Figs 1, 6A). The axons could be followed up to

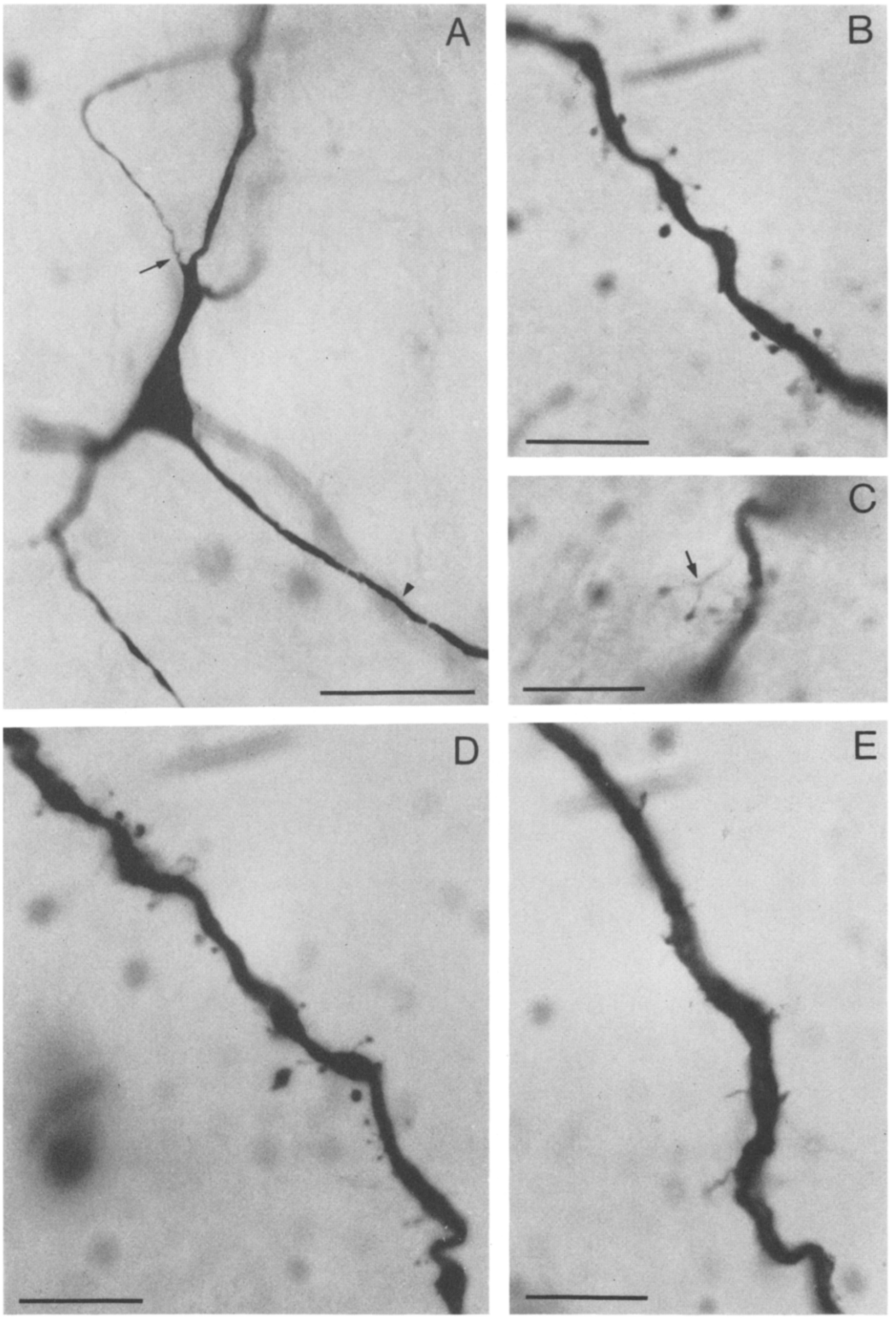

Fig. 6. Micrographs of the portions of cells 1–4 indicated by larger arrows in Figs 1–4. Orientations are as in Figs 1–4 unless otherwise noted. (A) The soma and proximal parts of cell 1. The presumptive axon is indicated by an arrow. Note the smooth appearance of a proximal dendrite (arrowhead); a more distal portion of the same dendrite is shown in E. Scale bar: 50 μm. (B) A dendrite and spines of cell 2. Scale bar: 10 μm. (C) A Y-shaped dendritic spine seen in cell 3. The arrow indicates the branching point of the Y. Scale bar: 10 μm. (D) A dendrite and dendritic spines of cell 4. Note the variety seen in the length of shaft and the size of head. The micrograph is oriented so that the proximal portion of the dendrite is at the lower right corner. Scale bar: 10 μm. (E) A distal part of the dendrite of cell 1 indicated by arrowhead in A. Note occasional appendages, which do not have distal heads. Scale bar: 10 μm.

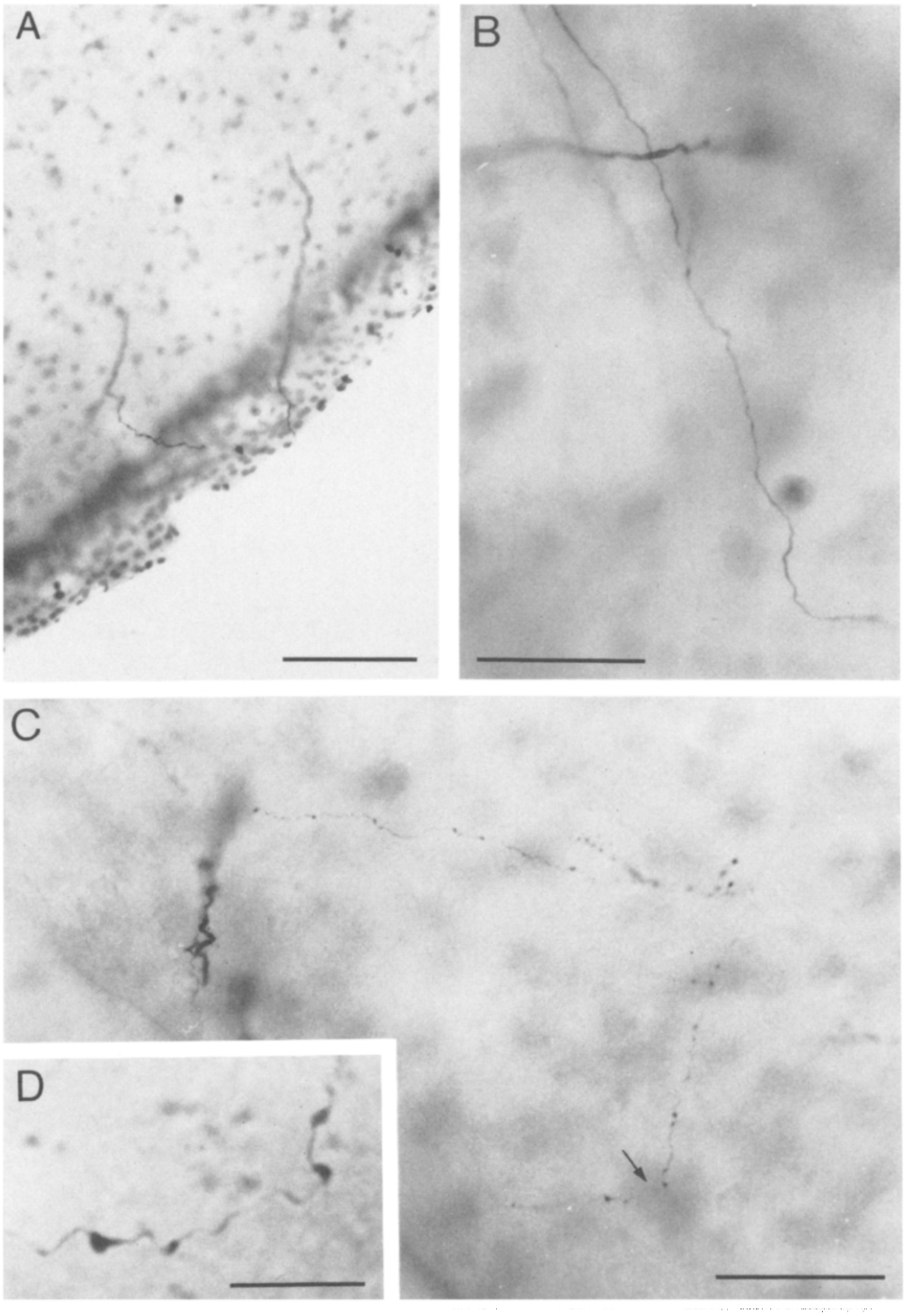

Fig. 7. Micrographs of the portions of cells 1 and 2 indicated by larger arrows in Figs 1 and 2. Orientations are as in Figs 1–4. (A) A dendrite of cell 2 in close vicinity of the ventral surface of the brain. The distal end of this dendrite in this micrograph was seen in an adjacent section to extend further for some distance along the ventral surface. This section was 100 μm in thickness, and one of the two surfaces of the section is in focus in this micrograph; the other surface is unfocused, thus appearing as a grey band in parallel with the section surface this is in focus. The section was counterstained with Cresyl Violet. Scale bar: 100 μm. (B) Axon branches of cell 1. Note the smooth appearance of the axon branches. The labelled process running horizontally is a dendrite. Scale bar: 50 μm. (C) Axon branches of cell 2 displaying occasional bouton-like swellings. The portion indicated by the arrow is shown at a higher magnification in (D). The thick labelled process on the left is a segment of dendrite. Scale bar: 50 μm. (D) Examples of bouton-like swellings seen in (C). Scale bar 10 μm.

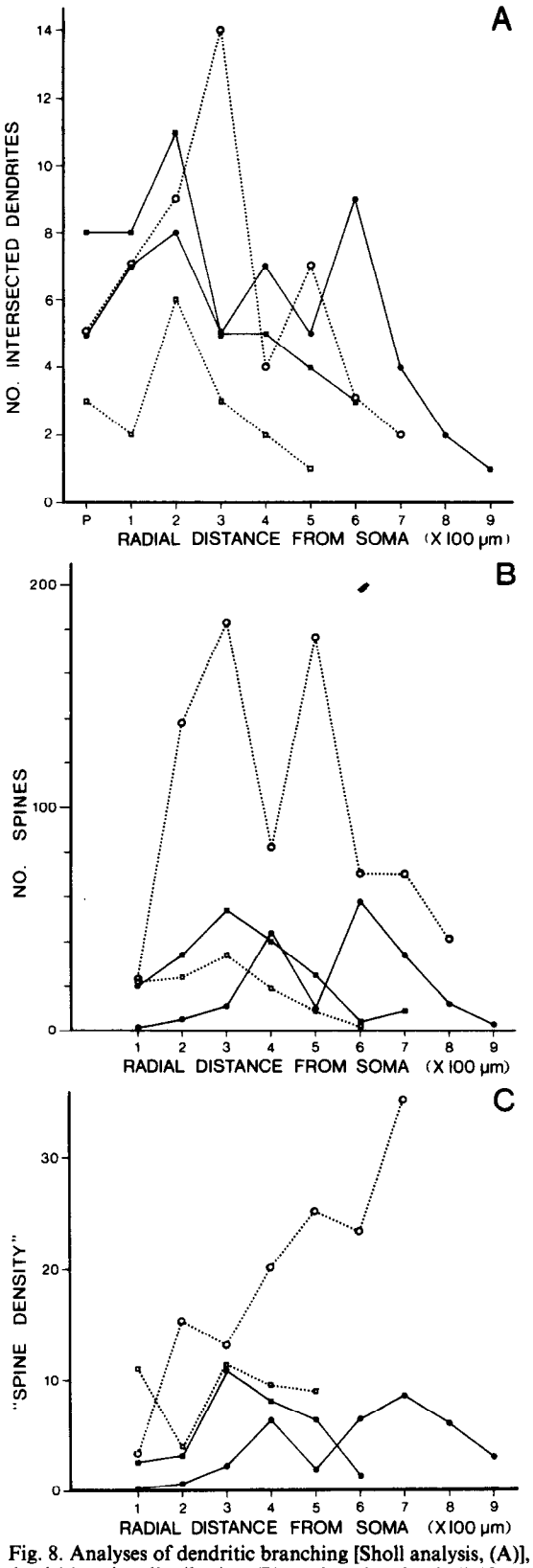

Fig. 8. Analyses of dendritic branching [Sholl analysis, (A)], dendritic spine distribution (B), and "spine density" (C) as a function of radial distance from the soma in cell 1 (●——●), cell 2 (○---○), cell 3 (■——■), and cell 4 (□---□). P on the abscissa in A indicates the number of primary dendrites. See Experimental Procedures for detailed procedures for each analysis.

about 500 μm from the soma (Figs 1, 2, and 4). In cell 1 (Figs 1, 7B) and cell 2 (Figs 2, 7C, 7D), some axon collaterals were seen within the dendritic field of the parent cell. Some of these collaterals displayed occasional varicosities, suggestive of boutons *en passant* (Fig. 7C, D). In cell 4 in the horizontal limb, the axon could be seen to make multiple turns, at about 90° at one point, until it disappeared as it coursed dorsally (Fig. 4). No collaterals were seen arising from this axon.

DISCUSSION

Technical considerations

As has been discussed previously,[4,22] the intracellular HRP technique is a powerful method for revealing the morphology of individual neurons, although it is not without problems. One of them is sampling bias towards a population of larger neurons. This happens because larger cells are easier to penetrate and hold, thus increasing the chance of obtaining better labelling. Therefore it is possible that the CPBF neurons in the present study were among the larger in the entire population of CPBF neurons.

A few cautions should be stated with regard to the final reconstructions of these neurons. First, although the morphology of reconstructed neurons was extensive, this should not be regarded as the entire morphology of these neurons, because: (1) some labelled neuronal elements, particularly some of those at the end of serial sections, were not included in the final reconstruction because they could not be unambiguously connected with those in previous sections, and (2) it is possible that some portions of these neurons (e.g. distal portions of dendrites) were not filled well with HRP.

The second caution regarding the reconstruction concerns tissue shrinkage, which affects both shape and dimensions of reconstructed neurons. Measurements reported in the present study were not corrected for tissue shrinkage; therefore these should be taken as underestimates. The effects of dehydration and clearing on the morphology of intracellularly labelled neurons have been examined recently by Grace and Llinás.[11] One of their obserations was that neuronal elements containing HRP-diaminobenzidine reaction product do not shrink as much as surrounding unlabelled neurons, and this difference in the degree of shrinkage can distort morphology. Consistent with this observation, in the present material HRP-labelled cells usually appeared much larger than Nissl-stained cells found in the surrounding tissue, and dendrites often showed bends and curls.

Morphological characteristics of cortically projecting basal forebrain neurons

Although the sample size is limited, the morphology of four CPBF neurons intracellularly labelled

in the present study is consistent with the previous observations using retrograde transport of HRP[7,12,14,19,24,26,38,39,50] or fluorescent tracers,[55,56] in that cortically projecting neurons in the basal forebrain are large multipolar neurons. In addition, the examination of intracellularly labelled CPBF neurons indicated that all four neurons have extensive dendritic fields, and display frequent dendritic spines. In spite of these common characteristics, however, some degree of heterogeneity was also present among the four CPBF neurons as discussed below. These morphological differences may be related to the physiological heterogeneity observed among CPBF neurons.[1a,25a,37]

The intracellularly labelled cells were located at different rostrocaudal levels in the basal forebrain, within the regions variably termed as the horizontal limb of the diagonal band, magnocellular preoptic area, and magnocellular basal nucleus.[2,26,40,48] These locations are consistent with previous anatomical findings in the rat on the distribution of cortically projecting neurons in the basal forebrain on the basis of retrograde labelling[7,12,14,19,24,26,38,39,50,55,56] as well as with the distribution of ChAT-immunoreactive[13,29,40] and acetylcholinesterase-containing neurons in the basal forebrain of the rat.[10,16,26,33,40] In the basal forebrain, ChAT-immunoreactive cells have been shown to contain acetylcholinesterase as well.[8,31,40] Although the transmitter used by the four CPBF neurons in the present study is unknown, previous anatomical studies indicated that all[2,55] or many[38,50,56] of CPBF neurons are cholinergic.

The size of soma was large; 30–50 μm in longest dimension in the four CPBF neurons. These sizes are slightly larger than those reported for basal forebrain neurons labelled for ChAT (20–35 μm),[1,5,13,40] or acetylcholinesterase (20–45 μm).[26,40] Although the sample size is limited, it is tempting to propose the following two explanations. One is that it is due to the sampling bias towards the population of larger cells, which is inherent in the intracellular HRP technique (see above). A second explanation is that HRP-labelled cells probably shrunk less during dehydration and clearing than did ChAT-positive cells. This is possible because the HRP–diaminobenzidine reaction product, the presence of which protects neuronal elements from shrinkage[11] (see above), is usually denser in cells labelled intracellularly with HRP than in cells immunolabelled for the presence of an antigen such as ChAT.

The somal size was slightly different among the four CPBF neurons at different rostrocaudal levels. That is, the two neurons (cells 3 and 4) located rostrally at the level of the anterior commissure decussation had smaller somata (28 and 33 μm) than those (42 and 52 μm) of the other two (cells 1 and 2), which were located caudally, at the level of the supraoptic nucleus. This is consistent with previous observations that ChAT-containing cells in the horizontal limb of the diagonal band tend to be smaller than those in the ventral pallidum and globus pallidus (15–40 vs 20–45 μm).[26,40] It is, however, also possible that this tendency does not reflect absolute differences in size, but, rather, the orientation of the soma and the plane of transection (in the present study, all the sections were cut coronally).

Examination of the dendritic arborization of CPBF neurons indicated that, although there were differences in the pattern of dendritic branching as well as in the size and orientation of dendritic field, all these neurons were multipolar cells with large dendritic fields. Their dendrites, tapering as they branched, extended from 600 to 900 μm in straight line length from the soma. The size of the dendritic field was positively correlated with the size of the soma in the four neurons.

The course of dendrites observed with cell 1 in the present study merits some discussion in light of observations made by Das and Kreutzberg[6] on Golgi-stained interstitial cells around the globus pallidus in rabbit and guinea pig. These authors suggested that these interstitial cells correspond to the cells which stain intensely for acetylcholinesterase, are cholinergic, and have cortical projections. However, according to their observations, the dendrites of these cells were confined within the internal capsule. In contrast, cell 1, located at the globus pallidus–internal capsule border, had some dendrites in the internal capsule, but many others in the globus pallidus. The discrepancy may be due to the different techniques used; for example, morphology obtained with the Golgi technique is usually more limited than that with the intracellular HRP technique, and the Golgi technique requires the use of premature animals for the best results and the morphology of their neurons may be different from that in adults.

The significance of dendritic branching patterns of CPBF neurons revealed by the Sholl analysis in the present study may be better appreciated by comparing the present results with the Sholl analysis of facial motoneurons intracellularly labelled with HRP in the cat (see Fig. 7 of Shaw and Baker[45]). Obviously the facial motoneurons are much larger; somal sizes are 37–65 μm in diameter, and the lengths of longest dendrites range from 800 to 1200 μm. At the peak of dendritic branching, which occurs around 400 μm from the soma, the number of intersected dendrites ranges from 19 to 28. An additional notable observation is that the facial motoneurons do not display spines. These morphological differences most likely reflect functional differences between CPBF neurons and facial motoneurons.

All of the intracellularly labelled CPBF neurons displayed dendritic spines, although their density varied. The presence of dendritic spines has been reported with Golgi-stained cells in the lateral preoptic area by Millhouse.[32] However, Das and Kreutzberg,[6] using the Golgi technique, observed that the interstitial cells around the globus pallidus had relatively few spines. The presence of dendritic

spines has been reported in the basal nucleus in studies using electron microscopy.[14,18,52]

Among the four labelled neurons, cell 2 displayed by far the greatest number of dendritic spines. An advantage of the intracellular HRP technique is that it affords the possibility of correlating physiological and morphological features. Physiological characterization prior to intracellular HRP iontophoresis indicated that cell 2 was a type II CPBF neuron as defined in a companion paper,[37] whereas the other three were type I CPBF neurons. Although the sample size is limited, it is interesting that the two physiologically defined subtypes of CPBF neuron display a morphological difference, with type II CPBF neurons having more spines than do type I CPBF neurons. It is, however, at present not clear how the higher spine density in type II CPBF neurons is related to their physiological features including the apparent loss of the somatodendritic portion of the antidromic action potential with high frequency stimulation and longer antidromic latencies.

Although not seen in all the CPBF neurons labelled with HRP, the presence of local axon collaterals displaying bouton-like swellings in some of these neurons suggests that the output of basal forebrain projection neurons may be directed locally as well as to distant sites. Local postsynaptic neurons may include interneurons or other CPBF neurons. Similar local collaterals have also been seen in neurons in the nucleus of the diagonal band following local injection of an anterograde tracer, *Phaseolus vulgaris* leucoagglutinin.[3]

The morphology of cell 1, located at the globus pallidus–internal capsule border, appears similar to that of globus pallidus neurons intracellularly labelled with HRP by Park *et al.*[34] in terms of large somal sizes and relatively unbranching, extensive dendrites. However, the similarity may be limited to that at the light microscopic level. Ingham *et al.*[14] examined the morphology of neurons in the medial globus pallidus and ventral pallidum that were double-labelled by retrograde HRP tracing from the cerebral cortex and ChAT immunohistochemistry. These double-labelled neurons had large somata and multiple dendrites which were relatively unbranched and smooth, the characteristics that are consistent with cell 1 in the present study as well as intracellularly labelled globus pallidus cells described by Park *et al.*[34] When examined at the electron microscopic level, however, the double-labelled cells were found to receive relatively few synaptic contacts on the soma as well as on proximal dendrites, whereas globus pallidus neurons that were neither HRP- nor ChAT-positive were ensheathed by a layer of axonal terminals, consistent with electron microscopic observations of HRP-injected globus pallidus cells.[9] It is evident that neurons with similar light-microscopic features can display very different synaptic connectives.

Although the synaptic connectivity of CPBF neurons labelled intracellularly with HRP remains to be examined, the observation by Ingham *et al.*[14] that cholinergic basal forebrain neurons projecting to the cortex receive relatively few synaptic contacts to the soma and proximal dendrites is important in understanding the significance of the morphology we observed in our HRP-labelled CPBF neurons. Sparse synaptic contacts to the soma and proximal dendrites have also been reported with unidentified basal forebrain neurons[18] and basal forebrain neurons retrogradely labelled from the cortex.[52] In contrast, frequent synaptic contacts have been seen on distal dendrites and spines of unidentified basal forebrain neurons.[18] Presumed corticofugal fibers have also been reported to contact distal dendrites more frequently than soma or proximal dendrites of cortically projecting neurons in the basal forebrain.[27] ChAT-containing basal forebrain neurons have been shown to receive synaptic contacts from amygdalofugal axons on dendrites[57] and from substance-P-containing boutons on the soma and dendrites.[15] In combination with these observations, the present finding of the extensive dendritic field and the presence of dendritic spines (especially distally) suggest that the major synaptic input to CPBF neurons may be received at distal dendrites and spines.

CONCLUSION

We have described the morphology of CPBF neurons intracellularly labelled with HRP following physiological identification and characterizations. Major morphological characteristics include large (30–50 μm) somal size, multiple (3–8) primary dendrites, extensive dendritic fields, and frequent dendritic spines. With these features in common, however, some variabilities were also seen among different CPBF neurons, which may be related to the physiological heterogeneity observed among CPBF neurons. The observation of large dendritic fields and frequent dendritic spines, in combination with previous findings on the synaptic connectivity of basal forebrain neurons, suggests that the major synaptic input to CPBF neurons may be delivered to their distal dendrites and spines.

Acknowledgements—We thank David Egger and John Steeves for generous loans of equipment, Steven Vincent for helpful comments on an early version of the manuscript, and Stella Atmadja and Joane Suzuki for photographic assistance. This research was supported by the Medical Research Council of Canada (MT-4674 and PG-0033). PBR is an MRC Fellow.

REFERENCES

1. Armstrong D. M., Saper C. B., Levey A. I., Wainer B. H. and Terry R. D. (1983) Distribution of cholinergic neurons in rat brain: demonstrated by the immunohistochemical localization of choline acetyltransferase. *J. comp. Neurol.* **216,** 53–68.

1a. Aston-Jones G., Shaver R. and Dinan T. G. (1984) Cortically projecting nucleus basalis neurons in rat are physiologically heterogeneous. *Neurosci. Lett.* **46,** 19–24.
2. Bigl V., Woolf N. J. and Butcher L. L. (1984) Cholinergic projections from the basal forebrain to frontal, parietal, temporal, occipital, and cingulate cortices: a combined fluorescent tracer and acetylcholinesterase analysis. *Brain Res. Bull.* **8,** 727–749.
3. Brashear H. R., Zahm D. S. and Heimer L. (1985) Local projections within the diagonal band demonstrated by anterograde transport of *Phaseolus vulgaris*-leucoagglutinin (PHA-L). *Soc. Neurosci. Abstr.* **11,** 200.
4. Brown A. G. and Fyffe R. E. W. (1984) *Intracellular staining of mammalian neurons.* Academic Press, London.
5. Butcher L. L., Gould E. and Woolf N. J. (1985) Morphologic characteristics of central cholinergic neurons in the rat. *Soc. Neurosci. Abstr.* **11,** 1238.
6. Das G. D. and Kreutzberg G. W. (1969) Evaluation of interstitial nerve cells in the central nervous system: a correlative study using acetylcholinesterase and Golgi techniques. *Ergebn. Anat. EntwGesch.* **41,** 1–58.
7. Divac I. (1975) Magnocellular nuclei of the basal forebrain project to neocortex, brain stem, and olfactory bulb. Review of some functional correlates. *Brain Res.* **93,** 385–398.
8. Eckenstein F. and Sofroniew M. V. (1983) Identification of central cholinergic neurons containing both choline acetyltransferase and acetylcholinesterase and of central neurons containing only acetylcholinesterase. *J. Neurosci.* **3,** 2286–2291.
9. Falls W. M., Park M. R. and Kitai S. T. (1983) An intracellular HRP study of the rat globus pallidus. II. Fine structural characteristics and synaptic connections of medially located large GP neurons. *J. comp. Neurol.* **220,** 229–245.
10. Fibiger H. C. (1982) The organization and some projections of cholinergic neurons of the mammalian forebrain. *Brain Res. Rev.* **4,** 327–388.
11. Grace A. A. and Llinás R. (1985) Morphological artifacts induced in intracellularly stained neurons by dehydration: circumvention using rapid dimethyl sulfoxide clearing. *Neuroscience* **16,** 461–475.
12. Henderson Z. (1981) A projection from acetylcholinesterase-containing neurones in the diagonal band to the occipital cortex of the rat. *Neuroscience* **6,** 1081–1088.
13. Houser C. R., Crawford G. D., Barber R. P., Salvaterra P. M. and Vaughn J. E. (1983) Organization and morphological characteristics of cholinergic neurons: an immunohistochemical study with a monoclonal antibody to choline acetyltransferase. *Brain Res.* **266,** 97–119.
14. Ingham C. A., Bolam J. P., Wainer B. H. and Smith A. D. (1985) A correlated light and electron microscopic study of identified cholinergic basal forebrain neurons that project to the cortex in the rat. *J. comp. Neurol.* **239,** 176–192.
15. Ingham C. A., Bolam J. P., Wainer B. H. and Smith A. D. (1985) Cholinergic basal forebrain neurons with reference to their afferent and efferent connections: a correlated light and electron microscopic study. *Neurosci. Lett.* **9,** S55.
16. Jacobowitz D. M. and Palkovits M. (1974) Topographic atlas of catecholamine and acetylcholinesterase-containing neurons in the rat brain. I. Forebrain (telencephalon, diencephalon). *J. comp. Neurol.* **157,** 13–28.
17. Jones E. G., Burton H., Saper C. B. and Swanson L. W. (1976) Midbrain, diencephalic and cortical relationships of the basal nucleus of Meynert and associated structures in primates. *J. comp. Neurol.* **167,** 385–420.
18. Juraniec J. (1979) Basal nucleus of Meynert. *Folia Morph.* **38,** 217–225.
19. Kievet J. and Kuypers H. G. J. M. (1975) Basal forebrain and hypothalamic connections to the frontal cortex and parietal cortex in the rhesus monkey. *Science* **187,** 660–662.
20. Kimura H., McGeer P. L., Peng F. and McGeer E. G. (1980) Choline acetyltransferase containing neurons in rodent brain demonstrated by immunohistochemistry. *Science* **208,** 1057–1059.
21. Kimura H., McGeer P. L., Peng F. and McGeer E. G. (1981) The central cholinergic system studied by choline acetyltransferase immunohistochemistry in the cat. *J. comp. Neurol.* **200,** 151–201.
22. Kitai S. T. and Bishop G. A. (1981) Horseradish peroxidase: intracellular staining of neurons. In *Neuroanatomical Tract-tracing Methods* (eds Heimer L. and RoBards M. J.), pp. 263–277. Plenum Press, New York.
23. Kristt D. A., McGowan R. A. Jr., Martin-MacKinnon N. and Solomon J. (1985) Basal forebrain innervation of rodent neocortex: studies using acetylcholinesterase histochemistry, Golgi and lesion strategies. *Brain Res.* **337,** 19–39.
24. Lamour Y., Dutar P. and Jobert A. (1982) Topographic organization of basal forebrain neurons projecting to the rat cerebral cortex. *Neurosci. Lett.* **34,** 117–122.
25. Lamour Y., Dutar P. and Jobert A. (1984) Cortical projections of the nucleus of the diagonal band of Broca and of the substantia innominata in the rat: an anatomical study using the anterograde transport of a conjugate of wheat germ agglutinin and horseradish peroxidase. *Neuroscience* **2,** 395–408.
25a. Lamour Y., Dutar P., Rascol O. and Jobert A. (1986) Basal forebrain neurons projecting to the rat frontoparietal cortex: electrophysiological and pharmacological properties. *Brain Res.* **362,** 122–131.
26. Lehmann J., Nagy J. I., Atmadja S. and Fibiger H. C. (1980) The nucleus basalis magnocellularis: the origin of a cholinergic projection to the neocortex of the rat. *Neuroscience* **5,** 1161–1174.
27. Lemann W. and Saper C. B. (1985) Evidence for a cortical projection to the magnocellular basal nucleus in the rat: an electron microscopic axonal transport study. *Brain Res.* **334,** 339–343.
28. McKinney M., Coyle J. T. and Hedreen J. C. (1983) Topographic analysis of the innervation of the rat neocortex and hippocampus by the basal forebrain cholinergic system. *J. comp. Neurol.* **217,** 103–121.
29. Mesulam M.-M., Mufson E. J., Wainer B. H. and Levey A. I. (1983) Central cholinergic pathways in the rat: an overview based on an alternative nomenclature (Ch1–Ch6). *Neuroscience* **4,** 1185–1201.
30. Mesulam M.-M., Mufson E. J., Levey A. I. and Wainer B. H. (1983) Cholinergic innervation of cortex by the basal forebrain: cytochemistry and cortical connections of the septal area, diagonal band nuclei, nucleus basalis (substantia innominata), and hypothalamus in the rhesus monkey. *J. comp. Neurol.* **214,** 170–197.
31. Mesulam M.-M., Mufson E. J., Levey A. I. and Wainer B. H. (1984) Atlas of cholinergic neurons in the forebrain and upper brainstem of the macaque based on monoclonal choline acetyltransferase immunohistochemistry and acetylcholinesterase histochemistry. *Neuroscience* **12,** 669–686.
32. Millhouse O. E. (1969) A Golgi study of the descending medial forebrain bundle. *Brain Res.* **15,** 341–363.
33. Parent A., Gravel, S. and Oliver A. (1979) The extrapyramidal and limbic systems' relationship at the globus pallidus level: a comparative histochemical study in the rat, cat, and monkey. In *Advances in Neurology* (eds Poirier L. J., Sourkes T. L. and Bedard P. J.), Vol. 24, pp. 1–11. Raven Press, New York.

34. Park M. R., Falls W. M. and Kitai S. T. (1981) An intracellular HRP study of the rat globus pallidus. I. Responses and light microscopic analysis. *J. comp. Neurol.* **211,** 284–294.
35. Paxinos G. and Watson C. (1982) *The Rat Brain in Stereotaxic Coordinates.* Academic Press, New York.
36. Price J. L. and Stern R. (1983) Individual cells in the nucleus basalis–diagonal band complex have restricted axonal projections to the cerebral cortex in the rat. *Brain Res.* **269,** 352–356.
37. Reiner P. B., Semba K., Fibiger H. C. and McGeer E. G. (1987) Physiological evidence for subpopulations of cortically projecting basal forebrain neurons in the anesthetized rat. *Neuroscience* **20,** 629–636.
38. Rye D. B., Wainer B. H., Mesulam M.-M., Mufson E. J. and Saper C. B. (1984) Cortical projections arising from the basal forebrain: a study of cholinergic and noncholinergic components employing combined retrograde tracing and immunohistochemical localization of choline acetyltransferase. *Neuroscience* **13,** 627–643.
39. Saper C. B. (1984) Organization of cerebral cortical afferent systems in the rat. I. Magnocellular basal nucleus. *J. comp. Neurol.* **222,** 313–342.
40. Satoh K., Armstrong D. M. and Fibiger H. C. (1983) A comparison of the distribution of central cholinergic neurons as demonstrated by acetylcholinesterase pharmacohistochemistry and choline acetyltransferase immunohistochemistry. *Brain Res. Bull.* **11,** 693–720.
41. Satoh K. and Fibiger H. C. (1985) Distribution of central cholinergic neurons in the baboon (*Papio papio*). I. General morphology. *J. comp. Neurol.* **236,** 197–214.
42. Satoh K. and Fibiger H. C. (1985) Distribution of central cholinergic neurons in the baboon (*Papio papio*). II. A topographic atlas correlated with catecholamine neurons. *J. comp. Neurol.* **236,** 215–233.
43. Semba K., Masarachia P., Malamed S., Jacquin M., Harris S., Yang G. and Egger M. D. (1983) An electron microscopic study of primary afferent terminals from slowly adapting type I receptors in the cat. *J. comp. Neurol.* **221,** 466–481.
44. Semba K., Reiner P. B., McGeer E. G. and Fibiger H. C. (1985) Cortically projecting magnocellular basal forebrain neurons in the rat. II. Morphology. *Soc. Neurosci. Abstr.* **11,** 1238.
45. Shaw M. D. and Baker R. (1985) Morphology of motoneurons in a mixed motor pool of the cat facial nucleus that innervate orbicularis oculis and quadratus labii superioris, stained intracellularly with horseradish peroxidase. *Neuroscience* **14,** 627–643.
46. Sholl D. A. (1953) Dendritic organization in the neurons of the visual and motor cortices of the cat. *J. Anat.* **87,** 387–407.
47. Shute C. C. D. and Lewis P. R. (1967) The ascending cholinergic reticular systems: neocortical, olfactory and subcortical projections. *Brain* **90,** 497–520.
48. Swanson L. W. (1976) An autoradiographic study of the efferent connections of the preoptic region in the rat. *J. comp. Neurol.* **167,** 227–256.
49. Vincent S. R., Satoh K. and Fibiger H. C. (In press) The localization of central cholinergic neurons. *Prog. neuropsychopharmac. biol. Psychiat.*
50. Wahle P., Sanides-Buchholtz C., Eckenstein F. and Albus K. (1984) Concurrent visualization of choline acetyltransferase-like immunoreactivity and retrograde transport of neocortically injected markers in basal forebrain neurons of cat and rat. *Neurosci. Lett.* **44,** 223–228.
51. Wainer B. H., Levey A. I., Mufson E. J. and Mesulam M.-M. (1984) Cholinergic systems in mammalian brain identified with antibodies against choline acetyltransferase. *Neurochem. Int.* **6,** 163–182.
52. Walker L. C., Tigges M. and Tigges J. (1983) Ultrastructure of neurons in the nucleus basalis of Meynert in squirrel monkey. *J. comp. Neurol.* **217,** 158–166.
53. Walker L. C., Kitt C. A., DeLong M. R. and Price D. L. (1985) Noncollateral projections of basal forebrain neurons to frontal and parietal neocortex in primates. *Brain Res. Bull.* **15,** 307–314.
54. Wenk G. L., Cribbs B. and McCall L. (1984) Nucleus basalis magnocellularis: optimal coordinates for selective reduction of choline acetyltransferase in frontal neocortex by ibotenic acid injections. *Expl Brain Res.* **56,** 335–340.
55. Woolf N. J., Eckenstein F. and Butcher L. L. (1983) Cholinergic projections from the basal forebrain to the frontal cortex: a combined fluorescent tracer and immunohistochemical analysis in the rat. *Neurosci. Lett.* **40,** 93–98.
56. Woolf N. J., Eckenstein F. and Butcher L. L. (1984) Cholinergic systems in the rat brain: I. projections to the limbic telencephalon. *Brain Res. Bull.* **13,** 751–784.
57. Zaborszky L., Leranth Cs. and Heimer L. (1984) Ultrastructural evidence of amygdalofugal axons terminating on cholinergic cells of the rostral forebrain. *Neurosci. Lett.* **52,** 219–225.

(*Accepted* 9 *July* 1986)